Approximate model of sound source in consideration of evanescent waves in far-field acoustical holography

Ziteng WANG[1]; Diange YANG[2]; Feng MIAO; Rujia WANG; Junjie WEN; Xiaomin LIAN

State Key Laboratory of Automotive Safety and Energy, Department of Automotive Engineering, Tsinghua

University, Beijing 100084, China

ABSTRACT

Far-field acoustical holography methods reconstruct the sound fields mainly based on the simple point source model because of the loss of abundant information compared with near-field acoustical holography (NAH). It brings problems that the reconstructed sound sources are different from the actual measured sound sources especially because of the evanescent waves which attenuate rapidly in the near field. In the recent study, we establish the approximation formulation of evanescent wave propagation which suggests that evanescent wave can be considered as the interference of dipole model and quadrupole model with different weighting factors distributed on the incident wave-front. Without the evanescent wave component, the constructed sound sources are actually the components that are effective in the far-field and we proposed the concept of "far-field effective sound source" to show its physical meanings. With simulations and actual experiments with known speakers, the approximation method of sound source model is validated and the far-field acoustical holography has been improved to achieve more accurate quantitative reconstruction results. The study explored the evanescent wave which is hard to capture and for engineering practice, this research can give more accurate reconstruction as well as the approximation.

Keywords: Sound source model, Evanescent waves, Far-field acoustical holography
I-INCE Classification of Subjects Number(s): 75.7, 76.1.7

1. INTRODUCTION

Sound source identification is an important foundation for noise control because being able to know where the noise is generated and how it propagates can help to reduce the noise. Various methods are used in sound source identification and different types of microphone arrays are employed for localizing the noise sources (1, 2, 3). Beamforming and acoustical holography are two widely used methods in sound sources identification. Compared with beamforming method, acoustical holography has the decided advantage that it can achieve quantitative measurement and reconstruction. In 1980s, Williams and Maynard proposed and conducted relatively systematic studies on the principles and the experiments using the near-field acoustic holography (NAH) (4, 5). Although NAH methods achieve quantitative measurement, they cannot be applied in far-field sound source because of the limitation of measuring conditions. In 1990s, Williams extended the NAH theory to far-field acoustical holography theory (6, 7). In 1990s, Yang originally proposed acoustical holography based on Kirchhoff diffraction theory (KDAH) (8), which was inspired by the classical Kirchhoff diffraction principle in optics. In addition, Yang and Wang improved the KDAH method with de-dopplerization method in time-domain to achieve sound sources identification of moving vehicles at the speed of 117 km/h (9).

Although these acoustical holography methods can give quantitative reconstruction results of sound sources, there is still no systematic investigation on the mechanism and errors in quantitative reconstruction. A key difficulty in validating the quantitative accuracy of acoustical holography is the loss of evanescent wave component in sound sources, especially in far-field conditions. Evanescent wave attenuates so rapidly that the far-field microphone array cannot capture it at all. So it remains as a challenge to validate the quantitative accuracy of sound sources reconstructed with far-field

---

[1] zt-wang11@mails.tsinghua.edu.cn
[2] ydg@tsinghua.edu.cn

acoustical holography. In order to reveal the influence on experiment validation of evanescent wave component in sound sources, the method of approximation sound source modeling is proposed to calculate the evanescent wave component. In Musafir's study, evanescent waves obtained by the decomposition of the trace field generated by a source distribution of finite extent on an infinite surface generally do not have physical existence (10). Makris and Psaltisfield claimed that the evanescent waves decayed along the propagation direction could be considered as the result of interference between elementary oscillating dipole sources rather than point sources (11). Their study further suggested that evanescent wave could be considered as the interference of dipole model and quadrupole model with different weighting factors distributed on the incident wave-front. Without the evanescent wave component, the reconstructed sound sources are actually the components that are effective in the far-field, so the concept "far-field effective sound source" is proposed to show the physical meanings. With simulations and actual experiments with known sound source, the approximate model method of sound source is validated to achieve more accurate quantitative reconstruction results in far-field acoustical holography.

2. THEORY AND METHOD

2.1 Influence of evanescent wave on far-field acoustical holography

Waves radiated from the sound sources are composed of two parts: propagation waves and evanescent waves. As Fig. 1(a) shows, propagation wave travel from the (x, y) plane, but evanescent wave travel parallel to it with wavefronts in vertical planes parallel to the (y, z) plane, as Fig. 1(b) shows.

(a)   (b)
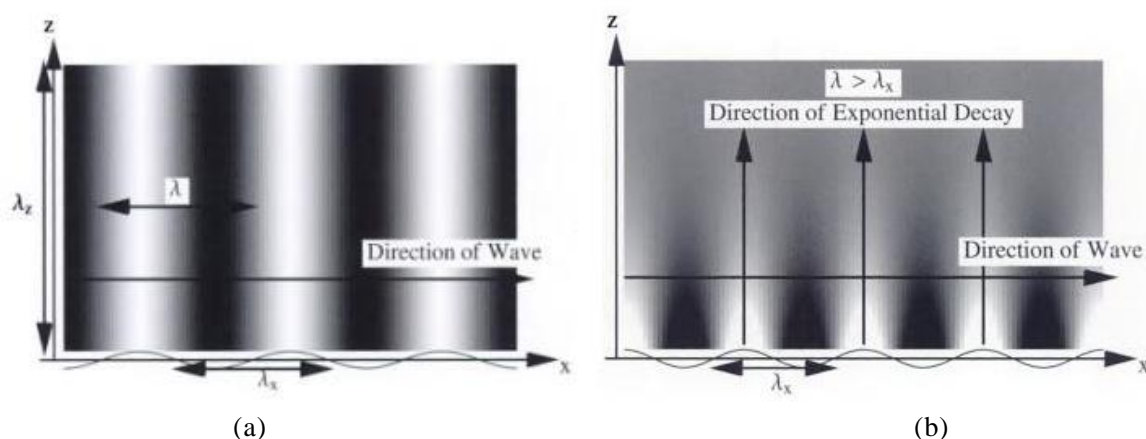
Figure 1 – The spectrum of propagation waves traveling and Evanescent waves traveling. (a) Propagation wave traveling parallel to x axis, infinite wavelength in the vertical direction. (b) Evanescent waves traveling parallel to x axis, decaying exponentially in the vertical direction.

The wavenumber in the three directions can be calculated from the constant wavelength k and two of them can be chosen as the independent variables. Here k_z is chosen as the dependent variable and calculated as Eq. (1) shows,

$$k_z = \pm\sqrt{k^2 - k_x^2 - k_y^2} \tag{1}$$

Since $k_y = 0$, particle motion is now only in the x direction. When k_z or k_y >k, Eq. (1) can be converted to Eq. (2). It is a condition under which the plane waves turn into evanescent waves.

$$k_z = \pm i\sqrt{k_x^2 + k_y^2 - k^2} = \pm i k_z' \tag{2}$$

Where k_z' is real and here it is restricted the solution to the decaying term according to Sommerfeld radiation condition and the evanescent waves is expressed as Eq. (3),

$$p = Ae^{-k_z' z} e^{i(k_x x + k_y y)} \tag{3}$$

Equation (3) is the form of an evanescent wave, exponentially decaying in amplitude in the z direction. When the evanescent waves travel more than the wavelength of the sound source λ, it decays and disappears. Near-field acoustical holography (NAH) method is applied under the condition that the measurement plane is much smaller than λ, which can capture the evanescent waves to reconstruct the sound source without the limitation of wavelength. In addition, evanescent waves conclude more information about the sound source such as particle velocity and vibration parameters, which make NAH can obtain more accurate results than far-field acoustical holography. In the research of Williams (12), the evanescent waves of NAH can be calculated as Eq. (4),

$$P(r) \approx (\frac{r_h}{r})^{n+1} P(r_h) \tag{4}$$

In Eq. (3), if all the sound sources are supposed contained within the minimum radius a, r_h is a greater radius ($r_h \geq a$) of a sphere where the hologram is obtained. $P(r)$ is the sound pressure at the propagation distance $d = r$, which is reconstructed from the sound pressure $P(r_h)$. However, far-field acoustical holography method was established based on the point sound source model. However, in the actual measurement, the influence of evanescent wave must be taken into consideration especially when the quantitative reconstruction is discussed. Without the proportion of evanescent wave component, the quantitative accuracy cannot be validated. Until now, there is no study that had discussed the physical meaning of the results reconstructed by far-field acoustical holography. The definition "far-field effective sound source" is proposed for this problem. Under the far field condition, the measured sound pressure can be regarded as the propagation of the sound source without the evanescent wave component. Because the acoustical holography reconstructs the sound source based on the far field sound signal without near-field evanescent component received by microphone array, the sound sources reconstructed by acoustical holography are actually the "far-field effective sound source".

2.2 Approximate model method for actual sound source

In order to calculate the influence of evanescent wave on quantitative accuracy, the evanescent wave component is considered in the classical and simple sound source model according to Morse acoustic theory, dipole source model and quadrupole source model. The resulting radiation field of dipole can be derived from that for simple source，the sound pressure of dipole can be expressed as Eq. (5),

$$p'(r,\theta,t) = -\frac{\cos\theta}{4\pi}\left[\frac{1}{c_0 r}\frac{\partial F}{\partial t} + \frac{F}{r^2}\right]\Bigg|_{t_r = t - r/c_0} \tag{5}$$

$-\dfrac{\cos\theta}{4\pi}$ is the propagation direction, the item $\dfrac{1}{c_0 r}\dfrac{\partial F}{\partial t}$ stands for the propagation wave component and $\dfrac{F}{r^2}$ stands for the evanescent wave component. If $F = Ae^{i\omega t}$, the sound pressure will be converted to Eq. (6),

$$p = \frac{Ae^{jkr}}{\pi}\left(\frac{i\omega}{c_0 r} + \frac{1}{r^2}\right)\cos\theta \tag{6}$$

When $\dfrac{\omega}{c_0 r} = \dfrac{1}{r^2}$, the propagation wave equals to the evanescent wave and the radiation radius is,

$$r_e = \frac{c_0}{\omega} = \frac{c_0}{2\pi f} \tag{7}$$

r_e is defined as the critical radiation radius. The proportion of evanescent wave in the dipole is calculated as Eq. (8),

$$\frac{P_{de}}{P_d} = \frac{\frac{1}{r^2}}{\frac{\omega}{c_0 r} + \frac{1}{r^2}} = \frac{c_0}{c_0 + \omega r} \tag{8}$$

The quadrupole sound source can be regarded as a combination of four simple sources, two of strength $+Q$, placed at the points $x = 1/2d, y = 1/2d, z = 0$ and $(-1/2d, -1/2d, 0)$, and two of strength $-Q$, placed at the points $(1/2d, -1/2d, 0)$ and $(-1/2d, 1/2d, 0)$. It's radiation sound pressure equation is as Eq. (9) shows,

$$p = -i\rho c k^3 Q_{xy} \frac{xy}{4\pi r^3} \left[1 + \frac{3i}{kr} - 3\left(\frac{1}{kr}\right)^2 \right] e^{ikr - i\omega t} \tag{9}$$

The proportion of evanescent wave in the dipole is calculated in Eq. (10),

$$\frac{P_{qe}}{P_q} = \frac{\frac{3}{kr} + 3\left(\frac{1}{kr}\right)^2}{\frac{3}{kr} + 3\left(\frac{1}{kr}\right)^2 + 1} = \frac{3kr + 3}{(kr)^2 + 3kr + 3} \tag{10}$$

With the propagation distance increases, the evanescent wave components of dipole source and quadrupole source is as shown in Fig. 2,

(a)   (b)
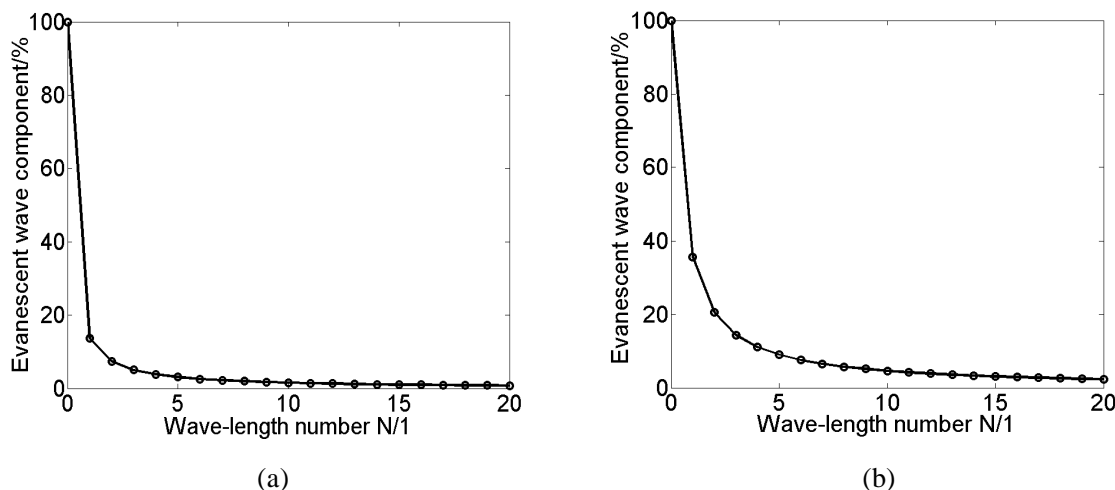
Figure 2 – Evanescent wave component proportion of dipole and quadrupole model

(a) diploe source, (b) quadrupole source

N is the wavelength number converted from propagation distance R. Figure 2 shows that when $N>3$, the evanescent wave component of diploe model is less than 5%; when $N>12$, the evanescent wave component of quadrupole model is less than 5%. It can be concluded that when the propagation distance d becomes longer, the evanescent wave component decay rapidly and can be ignored eventually in the sound pressure.

According to Morse acoustic theory, a real sound source can be regarded as a region vibrating sharply. If the region is small enough, the radiation wave from the sound source can be expressed as Eq. (11),

$$P_\omega(\mathbf{r}) = P_s(\mathbf{r}) + P_d(\mathbf{r}) + P_q(\mathbf{r}) \tag{11}$$

The equation suggests that real sound source can be regarded as a combination of single point source, dipole source and quadrupole source. Furthermore, the point source is so ideal that its weight in the actual sound source $p_s(\mathbf{r})$ is small. Depending on the rich experience from various measurement experiments on actual sound sources, actual sound source can be approximately decomposed into dipole source and quadrupole source with different weights. So it can be expressed as

Eq. (12),

$$P_\omega(\mathbf{r}) = W_d \cdot P_d(\mathbf{r}) + W_q \cdot P_q(\mathbf{r}) \tag{12}$$

W_d and W_q is the weighting factors of dipole source and quadrupole source. In the experiment, the approximate model of actual sound source can be built by the method above, W_d and W_q can be obtained by curve fitting. With the approximation model method described above, the influence and error caused by evanescent wave component can be calculated and eliminated.

3. EXPERIMENTS AND RESULTS

3.1 Evanescent wave component measurement and analysis

3.1.1 Experiment set up and measured sound source

In order to validate the approximation model method, experiments of actual sound source are carried out in the anechoic chamber. The actual sound sources measured in the experiments are volume sound source and HiVi loudspeaker as Fig. 3 shows. Linear uniform microphones are fixed to measure the 1000Hz single frequency volume of the sound source from very near to 2 meters. The effective sound pressure can be calculated. In order to illustrate the variation trend, the maximum amplitudes of measured sound source, dipole source and quadrupole source are normalized.

(a)   (b)
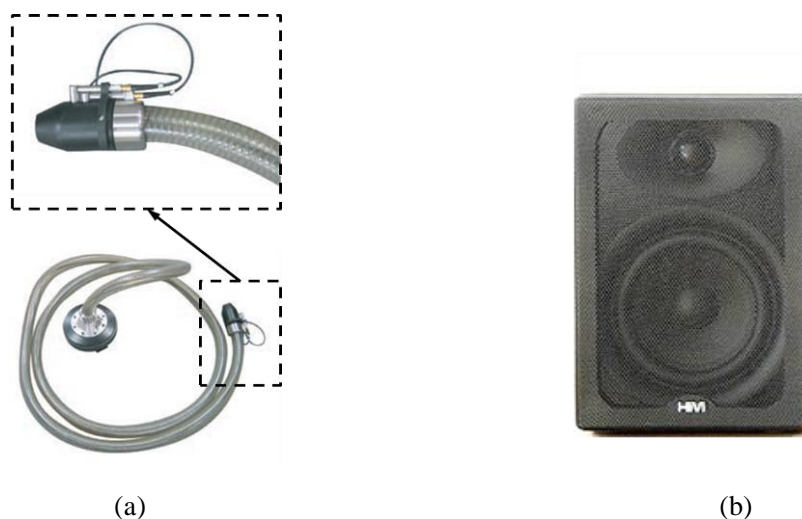
Figure 3 – Measured sound source (a) Volume sound source, (b) HiVi loudspeaker

3.1.2 Validation of approximation model for volume sound source

Some groups of volume sound source experiment results are shown in Table 1. The sound pressure curve of volume sound source at different measurement distance and the curve of normalized sound pressure of different sound source model with the wavelength number are shown in Fig. 4.

Table 1 – Sound pressure of volume source, dipole source and quadrupole source

Group	Propagation distance, m	Wavelength number	Dipole source pressure, Pa	Quadrupole source pressure, Pa	Measured sound pressure, Pa
1	0.19	0.559	1.000	1.000	1.000
2	0.33	0.971	0.576	0.331	0.476
3	0.55	1.618	0.345	0.119	0.302
4	0.72	2.118	0.264	0.070	0.239
5	0.12	3.441	0.162	0.026	0.150
6	0.15	4.294	0.130	0.017	0.089
7	0.19	5.647	0.099	0.010	0.042

(a)   (b)
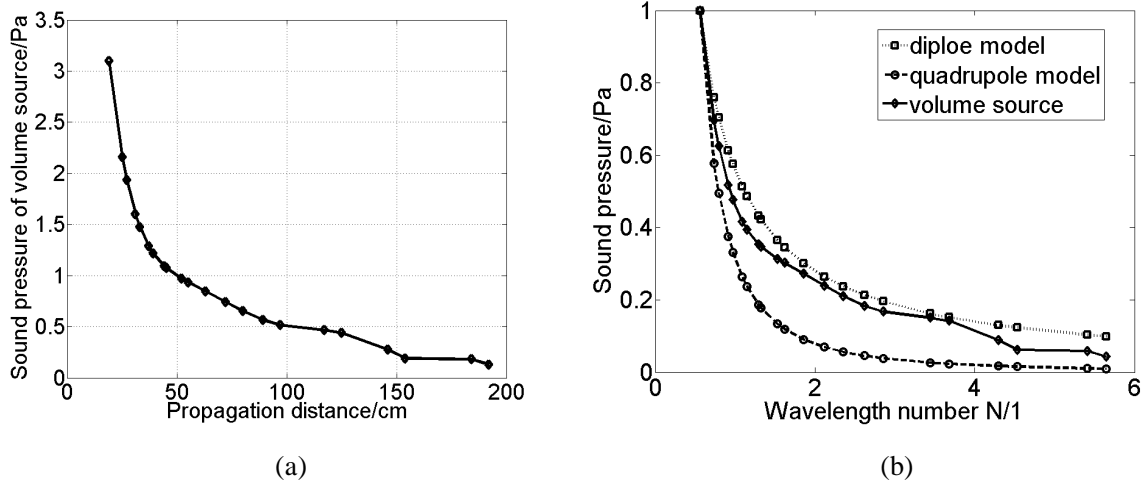
Figure 4 – Curve of sound pressure changed with the propagation distance (a) sound pressure curve of

volume sound source, (b) curve of normalized sound pressure of different sound source model

Based on the approximation model method mentioned above, the approximate model of the volume source is obtained by fitting the experimental data with the dipole source model and the quadrupole source model. If the sound pressure of volume source is $\mathbf{P_x}$, Eq. (13) is established to show the approximation model for volume source expressed in dipole source and quadrupole model. $\mathbf{P}_d$ is the sound pressure of the dipole source, $\mathbf{P_q}$ is the sound pressure of quadrupole source. W_d and W_q are the weighting coefficients.

$$\mathbf{P_x} = W_d \mathbf{P}_d + W_q \mathbf{P_q} \tag{13}$$

The equation is solved according to the following steps in Eq. (14),

$$\begin{bmatrix} p_{d1} & p_{q1} \\ p_{d2} & p_{q2} \\ \vdots & \vdots \\ p_{dn} & p_{qn} \end{bmatrix} \begin{bmatrix} W_d & W_q \end{bmatrix} = \begin{bmatrix} p_{x1} \\ p_{x2} \\ \vdots \\ p_{xn} \end{bmatrix}$$

$$\begin{bmatrix} p_{d1} & p_{d2} & \cdots & p_{dn} \\ p_{q1} & p_{q2} & \cdots & p_{qn} \end{bmatrix} \begin{bmatrix} p_{d1} & p_{q1} \\ p_{d2} & p_{q2} \\ \vdots & \vdots \\ p_{dn} & p_{qn} \end{bmatrix} \begin{bmatrix} W_d & W_q \end{bmatrix} = \begin{bmatrix} p_{d1} & p_{d2} & \cdots & p_{dn} \\ p_{q1} & p_{q2} & \cdots & p_{qn} \end{bmatrix} \begin{bmatrix} p_{x1} \\ p_{x2} \\ \vdots \\ p_{xn} \end{bmatrix} \tag{14}$$

$$\text{If } \mathbf{M}_{2\times2} = \begin{bmatrix} p_{d1} & p_{d2} & \cdots & p_{dn} \\ p_{q1} & p_{q2} & \cdots & p_{qn} \end{bmatrix} \begin{bmatrix} p_{d1} & p_{q1} \\ p_{d2} & p_{q2} \\ \vdots & \vdots \\ p_{dn} & p_{qn} \end{bmatrix}$$

$$\begin{bmatrix} W_d & W_q \end{bmatrix} = \mathbf{M}_{2\times2}^{-1} \begin{bmatrix} p_{d1} & p_{d2} & \cdots & p_{dn} \\ p_{q1} & p_{q2} & \cdots & p_{qn} \end{bmatrix} \begin{bmatrix} p_{x1} \\ p_{x2} \\ \vdots \\ p_{xn} \end{bmatrix}$$

The solution of the equation is $W_d = 0.73, W_q = 0.25$. The volume source approximation model is expressed as Eq. (15) and the comparison between approximation model and the actual sound source is shown in Fig. 4.

$$P_x = 0.727 P_d + 0.250 P_q \tag{15}$$

Obtained the approximation model in Eq. (15), fitting methods can be applied to further more optimize the model. In order to select the optimization fitting order, fitting models of different orders are established and calculated the fitting errors. The results of some fitting orders are shown in Fig. 5 and best performance is obtained when fitting order $n=6 \sim 8$.

(a) $n=2$	(b) $n=4$	(c) $n=6$
(a) $n=8$	(b) $n=10$	(c) $n=12$
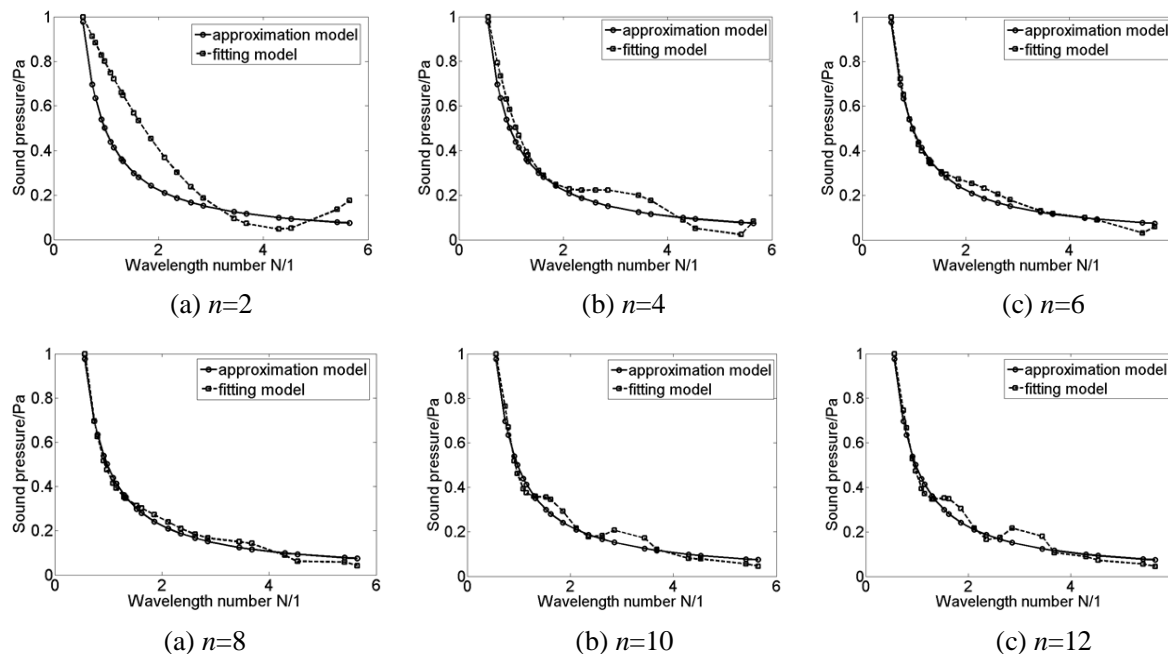
Figure 5 – Comparison between approximation models of different orders and real volume source

Figure 5 shows that the approximation model is close matched with the volume source curve and optimized fitting order can also improve the fitting degree.

3.1.3 Validation of approximation model for HiVi loudspeaker

Similar analysis procedure with volume sound source, its sound pressure propagation curve is shown and compared with dipole source and quadrupole source in Fig. 6.
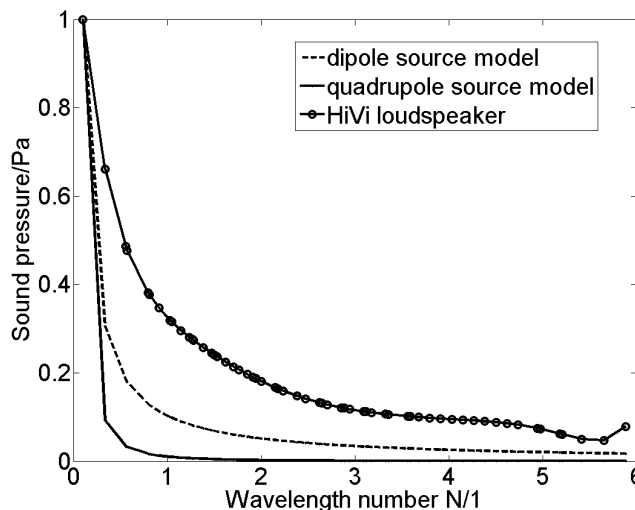
Figure 6 – Curve of HiVi loudspeaker sound pressure changed with the propagation distance

The HiVi loudspeaker sound pressure curve is not between the dipole source curve and the quadrupole source curve. This indicates that the evanescent wave component proportion in HiVi loudspeaker is greater than that in volume sound source. In order to apply approximation model method, the sound source can be regarded as the interference of some dipole sources, which means in Eq. (13) $W_q = 0$ and W_d is larger than 1. Figure 7 shows the approximation models when

W_d increase from 1 to 4. From the comparison results, it can be concluded that $W_d = 3$ is the optimization model for HiVi loudspeaker.

(a) $W_d = 1$ (b) $W_d = 2$

(c) $W_d = 3$ (d) $W_d = 4$
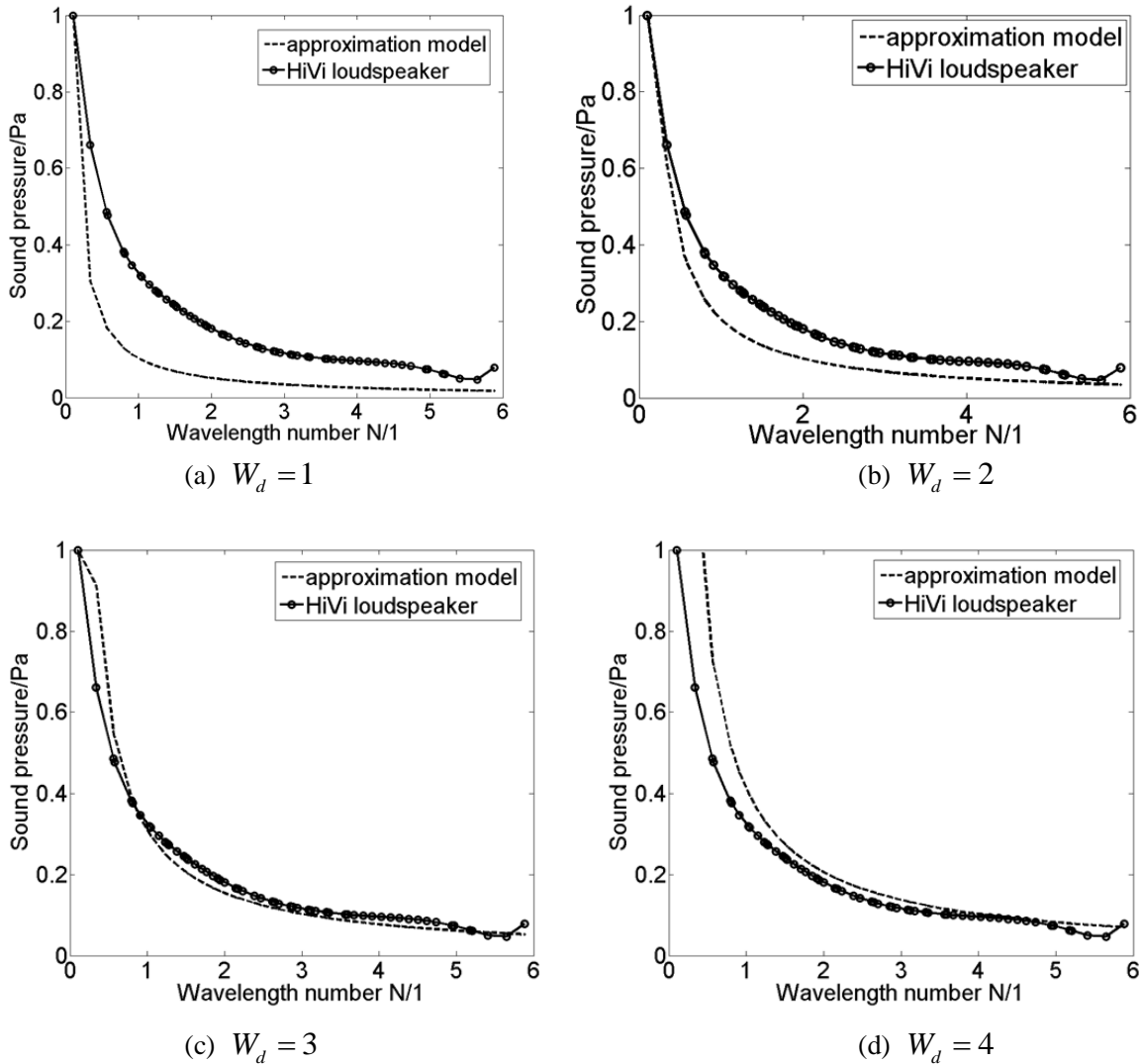
Figure 7 – Comparison between approximation models of different W_d and HiVi loudspeaker

Based on the approximation model method, we can approximately calculate the evanescent wave component at any position in front of the source. Sound pressure correction can also be achieved by this method. The development of the source approximation model method in our work will supply theoretical foundation for quantitative accuracy validation.

3.2   Far-field acoustical holography experiments and results

In order to validate the quantitative mechanism of far-field acoustical holography, a system is designed in our work to measure the volume sound source. The system is composed of X-shaped microphone array, two electronic cameras and a NI PXI data collector mentioned as in the previous section. The volume sound source plays 1000Hz single frequency harmonic sound. Microphone array composed of 21 microphones is located 1.8m in front of the loud speaker to measure the radiated sound pressure.

For the same experiment conditions, the locations of the volume source are identified and the near field sound pressure represented as the sound source is measured with the sound level meter. The sound pressure measured with sound level meter is taken as the reference value and it concludes the evanescent wave component. The result of sound source identification and reconstruction is shown in Fig. 8. The evanescent wave sound pressure at the position of the reconstructed sound source is calculated by the approximation model in Eq. (15).
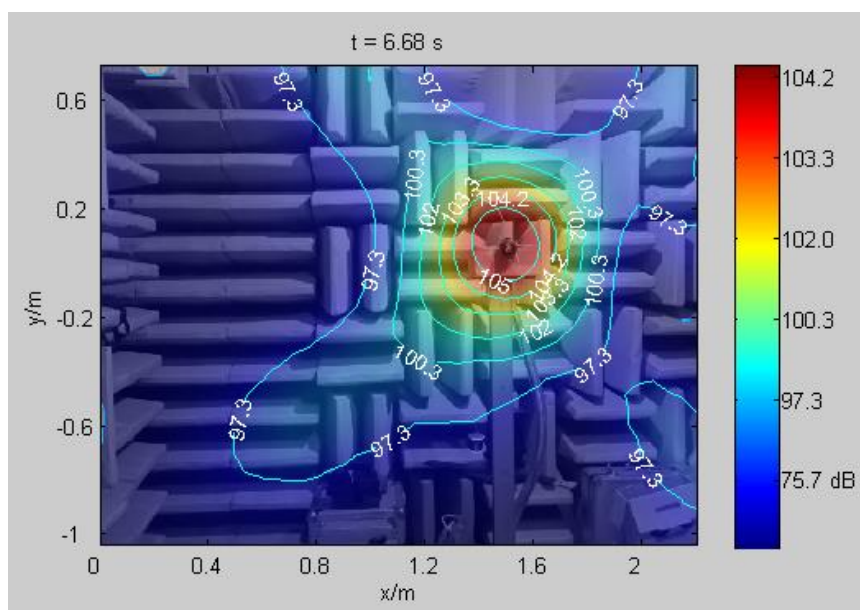
Figure 8 – Sound source identification and reconstruction result of far-field acoustical holography

Results show that the sound source reconstruction quantitative errors decrease by about 8%. These results prove that the sound source approximation model plays an effective role in correcting the evanescent wave error of point sound source model. Future research may focus on establishing an universally applicable method for establishing the approximate model of actual sound source needs to be proposed. In addition, the experiment results tell that holographic aperture is another critical factor on the quantitative accuracy of far-field acoustical holography.

4. CONCLUSIONS

In this paper, the influence of evanescent waves on the quantitative accuracy of far-field acoustical holography has been illustrated. Approximation model method for calculating evanescent waves component has been established based on dipole sound source model and quadrupole sound source model. Simulations and fitting curves show the effective performance of the approximation model. Experiment results with known sound source have demonstrated that this method can improve the quantitative accuracy of far-field acoustical holography more accurately. There still remain some further improvement in this method and the study will be continued in the future.

ACKNOWLEDGEMENTS

REFERENCES

1. Takano Y. Development of Visualization System for High-Speed Noise Sources with a Microphone Array and a Visual Sensor. Proc INTER-NOISE 03; 25-28 August 2003; Seogwipo, Korea 2003.
2. Sassaroli A, Castellini P, Giuseppe AD, Tomasini EP, Aversano M, Sollo A. Pass-by beamforming for airplane external noise characterization. Proc INTER-NOISE 10; 13-16 June; Lisbon, Portugal 2010.
3. Choi YC, Kim YH. Near field impulsive source localization in a noisy environment. J Sound Vib. 2007; 303: 209–220.
4. Maynard JD, Williams EG, Lee Y. Near field acoustic holography: I. Theory of generalized holography and the development of NAH. J Acoust Soc Am. 1985; 78 (4): 1395-1413.
5. Williams EG, Maynard JD. Holographic imaging without the wavelength resolution limit. Physical Review Letters. 1980; 45 (7): 554-557.
6. Williams EG. Supersonic acoustic intensity. J Acoust Soc Am. 1995; 97(1): 121-127.
7. Williams EG. Supersonic acoustic intensity on planar sources. J Acoust Soc Am. 1998; 104(5): 2845-2850.
8. Yang DG, Zheng SF, Li YK, Lian XM, Jiang XY. Research on acoustic holography method for the

identification of sound sources. Acta Acustica. 2001; 26(2): 156–160.

9. Yang DG, Wang ZT, Li B, Luo YG, Lian XM. Quantitative measurement of pass-by noise radiated by vehicles running at high speeds. J Sound Vib. 2011; 330: 1352-1364.

10. Musafir RE. On non-radiating sources. J Sound Vib. 2013; 332: 3947–3955.

11. Makris KG, Psaltis D. Huygens–Fresnel diffraction and evanescent waves. Opt Commun. 2011; 284: 1686-1689.

12. Williams EG. Fourier Acoustics: Sound Radiation and Nearfield Acoustical Holography. Naval Research Laboratory, Washington DC, USA: Academic Press; 1999.